JNeurosci
THE JOURNAL OF NEUROSCIENCE

Research Articles: Behavioral/Cognitive

Distinct patterns of connectivity between brain regions underlie the intra-modal and cross-modal value-driven modulations of the visual cortex

https://doi.org/10.1523/JNEUROSCI.0355-23.2023

Cite as: J. Neurosci 2023; 10.1523/JNEUROSCI.0355-23.2023

Received: 24 February 2023
Revised: 30 July 2023
Accepted: 26 August 2023

Distinct patterns of connectivity between brain regions underlie the intra-modal and cross-modal value-driven modulations of the visual cortex

Jessica Emily Antono[1], Shilpa Dang[1,2], Ryszard Auksztulewicz[3], Arezoo Pooresmaeili[1,4]*

[1] *Perception and Cognition Lab, European Neuroscience Institute Goettingen- A Joint Initiative of the University Medical Center Goettingen and the Max-Planck-Society, Germany, Grisebachstrasse 5, 37077 Goettingen, Germany*

[2] *School of Artificial Intelligence and Data Science, Indian Institute of Technology Jodhpur, Hauz Khas, New Delhi-110016, India*

[3] *Center for Cognitive Neuroscience Berlin, Free University Berlin, Habelschwerdter Allee 45, 14195 Berlin, Germany*

[4†] *School of Psychology, University of Southampton, University Road, Southampton SO17 1BJ, United Kingdom*

* Corresponding author: arezoo.pooresmaeili@gmail.com

† *Current Address*

Short title: BOLD signatures of intra- and cross-modal rewards

Number of pages: 35

Number of Figures: 4

Number of Tables: 2

Number of Extended Data Files: 3

Conflict of interests: The authors declare no competing interests.

Abstract

Past reward associations may be signalled from different sensory modalities; however, it remains unclear how different types of reward-associated stimuli modulate sensory perception. In this human fMRI study (female and male participants), a visual target was simultaneously presented with either an intra- (visual) or a cross-modal (auditory) cue that was previously associated with rewards. We hypothesized that depending on the sensory modality of the cues, distinct neural mechanisms underlie the value-driven modulation of visual processing. Using a multivariate approach, we confirmed that reward-associated cues enhanced the target representation in early visual areas and identified the brain valuation regions. Then, using an effective connectivity analysis, we tested three possible patterns of connectivity that could underlie the modulation of the visual cortex: a direct pathway from the frontal valuation areas to the visual areas, a mediated pathway through the attention-related areas, and a mediated pathway that additionally involved sensory association areas. We found evidence for the third model demonstrating that the reward-related information in both sensory modalities is communicated across the valuation and attention-related brain regions. Additionally, the superior temporal areas were recruited when reward was cued cross-modally. The strongest dissociation between the intra- and cross-modal reward-driven effects was observed at the level of the feedforward and feedback connections of the visual cortex estimated from the winning model. These results suggest that in the presence of previously rewarded stimuli from different sensory modalities, a combination of domain-general and domain-specific mechanisms are recruited across the brain to adjust the visual perception.

Keywords: reward, value, visual perception, sensory modality, fMRI

Significance Statement

Reward has a profound effect on perception, but it is not known whether shared or disparate mechanisms underlie the reward-driven effects across sensory modalities. In this human fMRI study, we examined the reward-driven modulation of the visual cortex by visual (intra-modal) and auditory (cross-modal) reward-associated cues. Using a model-based approach to identify the most plausible pattern of inter-regional effective connectivity, we found that higher-order areas involved in the valuation and attentional processing were recruited by both types of rewards. However, the pattern of connectivity between these areas and the early visual cortex was distinct between the intra- and cross-modal rewards. This evidence suggests

that to effectively adapt to the environment, reward signals may recruit both domain-general and domain-specific mechanisms.

Introduction

Rewards modulate information processing in the brain at multiple stages, from decision making where an organism's behavior is optimized to maximize reward outcomes (J. et al., 2001), to perception where the representations of sensory stimuli are altered depending on their current or past associations with rewards (Cicmil et al., 2015; Hickey et al., 2010; Rangel et al., 2008; Serences, 2008; Stanisor et al., 2013; Arsenault et al., 2013). Previous literature has demonstrated that a network encompassing the ventral striatum and prefrontal cortex plays a crucial role in learning and representation of reward value, thereby informing the subsequent decision-making stages about the best course of action to choose (Schultz, 2000; Rangel et al., 2008). On the other hand, a more recent line of research has provided evidence for a value-driven modulation of neuronal responses in almost all primary sensory areas (Rutkowski and Weinberger, 2005; Shuler and Bear, 2006; Pleger et al., 2008; Weil et al., 2010; Goltstein et al., 2013; Stanisor et al., 2013), a mechanism through which stimuli associated with higher rewards or better realization of the goals of the task are prioritized for perceptual processing. Despite the wealth of knowledge regarding the neuronal underpinnings of valuation in the brain and the emerging evidence for the value-driven alteration of perception, it is unclear how these processes interact.

Unravelling the mode of interaction between valuation and perception is a crucial step towards understanding how information processing in the brain is adapted to the rich and dynamic characteristics of the naturalistic environments. In such settings, objects have multiple features; from the same or different sensory modality; which may have different associations with rewards, and these associations may change over time. Therefore, to form a robust representation of reward value despite the multitude of stimulus features in the environment, the valuation network should constantly receive information from sensory areas (Komura et al., 2001; Reig and Silberberg, 2014). On the other hand, sensory areas should be efficiently re-regulated as reward associations of stimuli and task requirements undergo changes so that in each instance the stimuli that lead to better outcomes gain advantaged processing (Pessoa and Engelmann, 2010; Haber, 2011).

Different models have been put forward to explain the communication of information across the brain's valuation network and the sensory areas. Pessoa & Engelmann (2010) for

instance, proposed that reward signals are embedded into perceptual processing through either direct or indirect inputs from the valuation network to sensory areas. Direct inputs rely on a connectivity between the valuation network and sensory areas, whereas indirect inputs are likely to be first broadcasted to the frontoparietal attentional network (Corbetta and Shulman, 2002; Pessoa, 2009) and then be fed back to the sensory areas. Additionally, recent studies have identified other sensory association areas which may be involved in routing information between the valuation and perception networks. For instance, Pooresmaeili et al., (2014) found an increase of neural responses in the superior temporal cortex, known to be involved in multisensory processing (Calvert et al., 2000, 2001; Stein and Stanford, 2008), when auditory stimuli had been associated with higher rewards and modulated visual perception cross-modally. This finding suggested that areas involved in combining information across different features of a multisensory object may additionally integrate reward signals into the perceptual processing (Cheng et al., 2020). This proposal is also in line with the findings from another study (Anderson, 2017) showing that lateral occipital complex (LOC), an area that is involved in representation of perceived objects (Kourtzi and Kanwisher, 2001) and integration of local features to global shapes (Grill-Spector, 2003) especially when attention is biased to visual object features (Martin et al., 2018), plays a role in the value-driven changes in attentional control. Yet another possibility is that a history of privileged processing and preferred selection confers high reward stimuli a long-lasting processing gain already at the level of encoding of information at the early visual areas (Kim and Anderson, 2019), and hence value-driven modulation of perception occurs without the need for constant communication of information across the valuation and perception systems.

All mechanism outlined above have found support in the literature. For instance, direct inputs from the valuation network is plausible because previous studies have shown that lateral OFC and striatum have bilateral connections with the primary visual cortices (Barbas, 1993; Carmichael and Price, 1995; Kveraga et al., 2007; Khibnik et al., 2014). However, these connections may first be relayed to other areas as direct dopaminergic inputs to early visual areas such as area V1 are scarce (Oades and Halliday, 1987; Jacob and Nienborg, 2018) therefore supporting the proposal of a mediation through the sensory association (Macedo-Lima and Remage-Healey, 2021) or attentional (Noudoost and Moore, 2011) areas. The important role of attentional areas in mediation of value-driven effects is also supported by a host of previous studies (Pessoa, 2015), demonstrating that rewards guides attention to be allocated to the most valuable items in the scene (Chelazzi et al., 2013),

and attention in turn gates the effects of reward by determining whether or not rewarded stimuli are aligned with the goal of the task and should be boosted or supressed (Roelfsema and Van Ooyen, 2005; Roelfsema et al., 2010; Gong et al., 2017). Finally, an effect of reward locally arising at the level of sensory areas due to the reward history and its resultant long-lasting changes in sensory representations is supported by computational modelling (Wilmes and Clopath, 2019) and experimental approaches (Chubykin et al., 2013; Kim and Anderson, 2019) showing that during learning, the task-relevant neural representations that are predictive of rewards are locally boosted in area V1 (Poort et al., 2015).

The aim of the current study was to shed light on the underlying mechanisms of value-driven modulation of perception and the mode of interaction between the valuation and perception systems. Specifically, we sought to test which of the mechanisms mentioned above can best explain the value-driven modulation of visual perception across different types of reward-associated stimuli. Towards this aim, we used a behavioral paradigm similar to previous studies (Pooresmaeili et al., 2014; Antono et al., 2022; Vakhrushev et al., 2023) that featured either cross-modal (Pooresmaeili et al., 2014) or both cross- and intra-modal reward-associated stimuli (Antono et al., 2022; Vakhrushev et al., 2023). In this paradigm (**Figure 1**), auditory or visual stimuli were first associated with either high or low monetary reward during a reward associative learning phase (referred to as conditioning). During the test phase (post-conditioning), auditory and visual reward-associated stimuli (cross- and intra-modal, respectively) were presented at the same time as the target of a visual discrimination task but were irrelevant to the task at hand and did not predict the delivery of reward anymore. By having a comparison between intra- and cross-modal reward associated cues, we aimed to identify the reward-related mechanisms that are shared or disparate across the sensory modalities. Furthermore, to disentangle reward- and goal-related mechanisms, we associated rewards to the features of the stimulus that were not the target of the visual discrimination task. Concurrently as participants performed the behavioral task, we recorded the brain activity using fMRI.

We hypothesized that higher reward improves performance by enhancing the neural representation of the task target in the early visual areas. In our task, the visual discrimination had to be done on a target stimulus (i.e., a Gabor patch) while the reward-associated stimuli were presented simultaneously and at the same spatial location but were irrelevant to the task. Therefore, to examine the target-specific modulation of visual processing, we inspected how the accuracy of a multivariate pattern classifier for target's tilt orientation in the early visual

areas was influenced by the value of reward-associated stimuli. Furthermore, to identify which brain areas were engaged in encoding the associated reward value of stimuli, we used a second set of multivariate pattern classifiers that decoded stimulus value, either dependent or independent of specific sensory features, across the brain. Finally, we tested possible models of whether and how the long-range communication of reward information occurs between the valuation and early visual areas. Our results showed that overall higher reward enhanced the accuracy of target-specific representations in the early visual areas, but this effect involved distinct modes of long-range neuronal interactions across the brain for cross-modal and intra-modal reward-associated stimuli.

Materials and Methods

Participants

Thirty-six healthy participants were recruited (14 females; mean age 25.6 ± 4.48 SD, 20-40 years old) using an online local database (http://www.probanden.eni-g.de/orsee/public/). All participants had normal or corrected-to-normal vision, were right-handed, and gave oral and written informed consent after all procedures was explained to them. Three participants were excluded from all analyses since their performance in the reward conditioning task was below a pre-defined criterion (<80%) indicating that they could not localize the visual or auditory stimuli. One additional participant was excluded from the fMRI analysis since the data acquisition inside the scanner could not be completed (see the *Procedures*). Participants were paid 10€ per hour for their participation in 2 scanning sessions (each 2.5 hours), and in addition received a bonus up to 10€ depending on their performance. The study was approved by the local ethics committee of the "Universitätsmedizin Göttingen" (UMG), under the proposal number 15/7/15.

Stimuli and apparatus

The target stimuli used for the visual discrimination task (VDT, **Figure 1A, left panel**) were Gabor patches (a Gaussian-windowed sinusoidal grating with SD = 0.33°, a spatial frequency of 3 cycles per degree, subtending 2° diameter), which were tilted clockwise or counter-clockwise relative to the horizontal meridian. Gabor patches were displayed at 10° eccentricity to the left or right side of the fixation point and, in each trial, a semi-transparent ring (alpha 50%, 0.44° in diameter) was superimposed on them. The color of the rings (orange or blue for visual conditions, or grey for auditory and neutral conditions) was adjusted individually for each participant to make them perceptually isoluminant. For

auditory cues, two pure tones (600 Hz or 1000 Hz) were presented at 90dB simultaneously with the Gabor patch and at the same spatial location (see the *Procedures*). To achieve the co-localization of the auditory tones and the visual stimuli, we convolved the tones with head-related transfer functions based on a recorded database (Algazi et al., 2001) so that they could be perceived at 10° distance to the left or right of the fixation point. During the reward condition task (**Figure 1A, right panel**), only the orange or blue transparent rings or the auditory tones were presented (see also the **Procedures**).

Throughout the experiment, visual stimuli were displayed on an MR-compatible projection screen using a calibrated ProPixx projector (VPixx Technologies, Saint-Bruno, QC, Canada) at a resolution of 1920x1080 pixels, and a refresh rate of 120 Hz. The screen was placed at the end of the scanner bore at a distance of 88 cm from the participants' eyes. The full display size on the screen was 43 cm x 24 cm, i.e., the visible range from the central fixation spot was +/- 13.6° horizontally and +/-7.7° vertically. The auditory tones were delivered through MR compatible earphones (Sensimetric S15, Sensimetrics Corporation, Gloucester, MA) with an ear tip (Comply™ Foam Canal Tips) to maintain acoustic seal and reduce environmental noise.

For tracking the gaze position an MRC eye-tracker system mounted on the mirror on top of the MR head coil was used (MRC HiSpeed, MRC Systems GmbH, Heidelberg, Germany). Before each of the two scanning days, the eye-tracking system was calibrated using a 9-point standard MRC calibration procedure.

Procedures

The data collection was done over two scanning days (about 2.5 hours each). The first session consisted of a preparation phase (comprising a practice session for the visual orientation discrimination task: VDT, measurements of the sound localization, adjustment of colors' luminance and determining the perceptual threshold for the VDT) and an experimental phase referred to as pre-conditioning with the simultaneous acquisition of fMRI data.

Prior to the scanning, participants completed a sound localization task, where they had to indicate whether a sound was played from the left or right side using their index and middle finger on a keyboard and were included in the study if their localization accuracies were >95%. Afterwards, participants adjusted the luminance of both visual cues using a flicker task inside the scanner. The tilt orientation of the Gabor patch during the orientation

discrimination task was set to each participant's perceptual threshold estimated after the initial training and inside the scanner. To determine this threshold, we employed a QUEST algorithm (Watson and Pelli, 1983) to estimate the Gabor tilt orientation for which participants' performance was at 75%. Thresholds were determined when Gabors were superimposed with a grey circle.

The scanning session started with the pre-conditioning phase (320 trials) employing an orientation discrimination task (VDT) shown in **Figure 1A**. Each trial started with a fixation period (3000-5000 ms) followed by the presentation of the Gabor target (250 ms). Simultaneously with the target, either a visual or an auditory cue was presented (interleaved across trials). Participants were required to indicate whether the Gabor target was tilted clockwise or counter-clockwise relative to the horizontal meridian by pressing one of the two vertical buttons on a 4-button response pad (Current designs Inc., Philadelphia, PA). Participants' responses were considered valid if they occurred within a 2000 ms window after the offset of the Gabor. The response window was followed by the presentation of a feedback display for 500 ms. During the VDT task, the feedback display only contained the fixation point. The first scanning session terminated after the completion of pre-conditioning and participants attended the second session after at least 24 hours.

In the second scanning day, participants first completed a conditioning task to learn the reward associations of auditory and visual cues (see **Figure 1A, right panel**). During conditioning, participants were instructed to localize the visual (orange or blue rings) and auditory cues (pure tones 600 or 1000 Hz) and indicate whether they were presented to the left or to the right, by pressing one of the 2 horizontal buttons on a 4-buttons response pad. Upon correct response, participants saw the magnitude of the reward that was paired with a certain cue on the feedback display and thereby learned whether a visual or auditory stimulus was associated with high (mean = 25 Cents) or low (mean = 2 Cents, drawn from a Poisson distribution) monetary reward. Participants were instructed that they would get the sum of the monetary reward shown during this phase. In the final phase, referred to as post-conditioning (320 trials), the same procedure as in the pre-conditioning was employed with the exception that the task-irrelevant auditory (pure tones 600 or 1000 Hz) and visual cues (orange or blue rings) had already been associated with different amounts of monetary rewards. Additionally, in both pre- and post-conditioning phases, one additional condition referred to as the neutral condition was included. The neutral condition contained the Gabor target overlaid by a semi-transparent grey ring. Since the grey color was never associated with any reward value during

the conditioning, the neutral stimulus served to measure target-specific responses in the visual cortex. Participants were instructed that they would get a bonus for each correct response in the postconditioning phase, independent of the identity of the visual or auditory cues, though they would not be able to see the reward feedback.

In order to prevent extinction, we interleaved the post-conditioning blocks (each block with 40 trials) with a short conditioning block (8 trials, see **Figure 1B**). To ensure that participants had learned the reward-cue associations, we asked a question during and after the experiment. Based on these, all participants could correctly identify which cue properties were associated with high compared to low reward magnitudes.

Behavioural data analysis

The data obtained from all parts of the experiment was analysed using custom-written scripts in MATLAB (version R2015a). For the behavioural analysis, we removed the trials in which participants did not respond or had extreme response times. To determine the extreme response times, we first log transformed each participant's reaction times to achieve a roughly normal distribution and then removed trials which had reaction times >2SD from the mean (across all trials of each phase). This procedure removed 4.55, 4.67 and 5.13% of trials as outliers from the pre- and post-conditioning and conditioning, respectively. From the remaining trials, we calculated the mean of each response variable (accuracy and reaction times of correct trials) for each condition (high and low reward in auditory and visual cues) per subject during the post- and pre-conditioning separately. Afterwards, we entered the difference of accuracies and reaction times between the two phases (i.e., pre- and post-conditioning) as dependent variables into a 2x2 repeated measures ANOVA, with sensory modalities (intra- or cross-modal) and reward magnitude (high or low) as independent factors.

MRI data acquisition

The imaging data was collected using Siemens Magnetom Prisma Fit (3T) with a 64 channels head coil at the University Medical Centre Göttingen. Structural images were acquired for each session using a MPRAGE T1-weighted sequence (FOV: 256 x 256mm; voxel size: 1 x 1 x 1mm; TR: 2250ms; TE: 3.3ms; number of slices: 176). Functional images were acquired using an EPI sequence (TR: 900ms; TE: 30ms; FOV: 210 x 210mm; voxel size: 3 x 3 x 3mm; slice thickness: 3mm; flip angle: 60°; number of slices: 45).

fMRI data preprocessing

The imaging data was processed using the Statistical Parametric Mapping software (version SPM12: v7487; https://www.fil.ion.ucl.ac.uk/spm/). The data preprocessing pipeline consisted of realignment of the slices to the mean image, unwarping the images according to the voxel displacement mapped image, slice time correction for multiband interleaved sequence, coregistration between the functional and the structural images, segmentation of brain tissues according to the tissue probability maps, spatial normalization to the MNI space, and spatial smoothing with a kernel size of 8 mm (FWHM: 8 mm). All preprocessing steps were undertaken for the images that entered into the univariate GLM. For the multivariate analysis (MVPA), all steps were done except for the spatial normalization and spatial smoothing (see also under the *MVPA analysis*). For one participant the image required for unwarping could not be acquired due to technical problems at the scanner and we excluded this participant from all further fMRI analyses, resulting in N = 32 for the corresponding results.

Univariate GLM for effective connectivity

For the effective connectivity analysis, we specified a univariate General Linear Model (GLM) using the preprocessed functional images that were acquired during the two days of scanning in each participant. The univariate GML contained 51 event-related regressors convolved with the canonical hemodynamic response function (HRF). The events of interest were modelled using 10 regressors for each of the pre- and post-conditioning phases and 8 regressors for the conditioning phase. These regressors were stick functions time-locked to the onset of the stimulus presentation in each trial (**Figure 1A**) and corresponded to different experimental conditions varying in the reward magnitude (H-high or L-low), the sensory modality of the cues (V-visual or A-auditory), and the sides (L-left or R-right) for each phase. Furthermore, regressors modelling the neutral trials (N-neutral: with no reward association) on each side were included in the pre- and post-conditioning phases.

Additionally, we included the following regressors of no interest in the GLM: four regressors that modelled the presentation of the instruction displays, one regressor that marked the interleaved blocks of reward conditioning during the post-conditioning phase (**Figure 1B**), and four regressors for marking each period of data acquisition (i.e. one regressor for day 1 and three regressor for day 2, corresponding to the periods between the start and the end of the scan). Since the data of both days were modelled in a single GLM, a regressor marked each day (day 1: the pre-conditioning phase and day 2: the conditioning and

post-conditioning phases) and six regressors containing the estimated head motion parameters for each day were also added to the GLM for each day.

Multivariate analysis (MVPA)

For the MVPA analysis, we created a GLM where each trial in the pre- and post-conditioning was included as a separate regressor modelled with stick functions at the onset time of the target stimulus. The regressors of no interest and the reward conditioning phase in day 2 were modelled similarly to the univariate GLM and all regressors were convolved with the canonical haemodynamic response function (HRF). The parameter estimates of this GLM (t values) were then fed into several pattern classifiers using LibSVM's implementation of linear support vector machines (SVMs) (www.csie.ntu.edu.tw/~cjlin/libsvm). SVM classification was done using a whole-brain searchlight method, where the classification accuracy of each pattern classifier was computed based on the information contained in all voxels within a spherical searchlight region (radius: 6 mm) using a 10-fold cross-validation method. The searchlight was iteratively moved over every voxel in the whole-brain images and the calculated classification accuracy within each sphere was mapped to the voxel at the centre and normalized against the chance level accuracy (~ 50% for a two-class pattern recognition). The output of the classifiers was used to compute first-level contrast images (see the description of orientation and value decoders below), which were then spatially normalized to the MNI space and smoothed (FWHM, 3 mm). These contrast images were then entered into a second-level analysis, in which the statistical significance of each contrast was evaluated using one-sample t tests.

Our pattern classification analysis comprised two main types of decoders: *an orientation decoder* to classify the tilt orientation of the target stimulus (i.e., classifying clockwise or counterclockwise tilt orientation) and several *value decoders* to classify the associated reward magnitude of visual or auditory stimuli (i.e., classifying high or low reward magnitudes). These classifiers were designed to identify the early visual areas that encoded information about the target (orientation decoder) and brain regions that contained information about the associated reward value of stimuli (value decoders), respectively. Orientation decoders classified the stimulus orientation separately for different reward (high or low), cue modality (auditory or visual) and side (left or right). To examine the effect of reward value on early visual areas, we inspected the classification accuracy of this decoder using the contrast *High Value* > *Low Value* across all conditions (side and modality) during the post-conditioning corrected for the effects that existed prior to the learning of reward

associations during the pre-conditioning. To identify the regions that contained information about reward value after learning of reward values, we built 2 types of value decoders: 1) value decoders that classified stimulus value across all conditions (i.e., both modalities: auditory or visual and sides: left or right), and 2) value decoders that classified stimulus value separately for each sensory modality and each side. These decoders thus identified brain regions that were invariant to sensory modality and spatial location (*value decoder*$_1$) or were sensitive to sensory modality and spatial location (*value decoder*$_2$). The results of value decoders in post-conditioning were corrected against the results prior to the learning of reward associations in the pre-conditioning.

Effective connectivity analysis

In order to understand how cross- and intra-modal reward information is communicated across different brain regions to modulate the early visual areas, we set up an effective connectivity analysis using a dynamic causal modelling (DCM) approach (Friston et al., 2003). DCM is a model-based approach allowing us to test a set of a priori hypotheses regarding how learned reward associations are communicated across the brain to modulate visual target processing. The first hypothesized mechanism is based on a direct communication between the reward-related and the early visual areas, whereas the second mechanism relies on the involvement of either attention-related or sensory association areas to first process the reward information before it is further relayed to the early visual areas. Alternatively, reward-related information might be locally encoded in the early visual areas without the necessity of long-range communications across brain regions.

In order to test these hypotheses, we extracted the time series of the regions of interest (ROIs) that were identified by MVPA decoders (i.e., orientation and value decoders) treating them as nodes in DCM networks to be modelled. Both types of decoders could potentially identify multiple brain regions (see the Results and **Table 2**). Therefore, we limited our analysis to ROIs that were most informative for testing our a priori hypotheses. These ROIs comprised the early visual areas (EVA) known to contain information about the stimulus orientation (Hubel and Wiesel, 1968; Grill-Spector and Malach, 2004) and valuation areas that based on previous literature are known to play a role in coding stimulus value and attentional or sensory processing. The visual ROIs (see **Table 2**, **Figure 2B** and **Figure 2C**) were defined as regions that had a significantly higher orientation classification accuracy in the presence of high compared to low reward stimuli across both modalities (i.e. the contrast: *High Value* > *Low Value*) in post- compared to pre-conditioning and were within an

anatomical mask consisting of bilateral V1-V2 areas (Eickhoff et al., 2005). In order to define the ROIs that contained information about the stimulus associated value, we inspected the results of our two *value decoders* (see also the description of MVPA methods). The classification results of *value decoder*$_1$ revealed a right lateralized inferior orbitofrontal area ([51 26 -7], *p* uncorrected < .005, k = 20), an area known to encode the associated value of stimuli (Kringelbach, 2005; Zald et al., 2014). The output of the *value decoder*$_2$ was inspected either across sensory modalities or based on an interaction contrast that tested whether a region contained more information about the associated value of a specific sensory modality over the other (e.g., classification accuracy is higher for auditory than visual). Among the activations revealed by the *value decoder*$_2$ (**see Table 2**), we selected two clusters: the strongest activation at the right superior temporal areas (STS; at [57 -28 8], *p* uncorrected < .005, k = 20) and the largest cluster that corresponded to the left anterior intraparietal sulcus (IPS; at [-33 -58 53], *p* uncorrected < .005, k = 20). STS has been consistently found to underlie multisensory processing (Calvert et al., 2000; Stein and Stanford, 2008) exhibiting reward modulation in a similar paradigm (Pooresmaeili et al., 2014). IPS is a region known to play a role in the allocation of attention (Corbetta et al., 2000; Corbetta and Shulman, 2002; Serences and Yantis, 2007) and has well-documented neuroanatomical connections with the frontal areas (Greenberg et al., 2012).

For each ROI, time series were extracted separately for pre- and post-conditioning by overlaying the group functional ROI on each participant's structural scan. Within this framework, we estimated 11 biologically plausible models for the pre- and post-conditioning phases in which the directed causal influences among brain regions could change by three types of parameters: driving inputs and intrinsic and modulatory connections. Driving inputs corresponded to the incoming visual information contained in the different experimental conditions. To estimate the driving inputs, we used the univariate GLM which provided us the estimated BOLD times series of our 5 experimental conditions: intra-modal high reward (VH), intra-modal low reward (VL), cross-modal high reward (AH), cross-modal low reward (AL), and neutral (N). For each driving input, the data of two sides (left and right) were fed to the DCM models. Furthermore, as all stimuli contained the same visual target (i.e., the Gabor patch), we fed all driving inputs into the visual ROI (EVA) which is the first stage of information processing in a visual task. Intrinsic (condition-independent) connections were defined between every pair of nodes in the network and as self-connections. The models differed from each other with respect to the modulatory connections, which varied with the

experimental conditions (**Figure 4**). In the null model, only intrinsic connections were included, and no condition-dependent modulatory connection existed. The rest of the models assumed different patterns of connectivity between the EVA and other ROIs. One class of models (model 1-4) assumed that the valuation ROI (i.e., lateral OFC) communicated with the early visual areas indifferently across the intra- and cross-modal conditions. Specifically, model 1 held that lateral OFC directly communicated the reward information with the EVA, which is plausible given that direct inputs from the visual and auditory cortices to the lateral OFC have been reported before (Kringelbach, 2005). Another possibility was that the communication between the valuation and visual ROIs is indirect, with the information being first relayed to sensory-related ROI for cross-modal condition (model 2). Specifically, these models involved a modulatory connectivity between OFC-STS (Zald et al., 2014) and thereafter from STS to EVA, comprising connectivity patterns that are supported by previous studies (Felleman and Van Essen, 1991; Lewis and Noppeney, 2010). The third possibility was that the valuation and visual ROIs influenced each other through engaging the attention-related areas, i.e., IPS in our case; (model 3) or both attentional and sensory areas (model 4). The pattern of inter-areal connectivity assumed by these models is in line with the previous literature showing functional and structural connectivity between these areas: lateral OFC is functionally connected with IPS (Zald et al., 2014), IPS has connections to STS (Bray et al., 2013) and early visual areas (Felleman and Van Essen, 1991; Bray et al., 2013), and has a domain-general function across sensory modalities (Lingnau et al., 2014). Moreover, STS has been known to have a functional connection with the primary visual area (Noesselt et al., 2007). So far, model 1-4 assumed that intra- and cross-modal cues behaved similarly. In order to capture the possibility of a dissociation between intra- and cross-modal pathways, we also modelled another class of models (model 5-10) where distinct pathways were involved in intra- and cross-modal reward processing. Lastly, we also included a *null* model (model 11), which assumed that the influence of reward on early visual areas occurred locally within these areas and did not require a constant long-range communication with other areas.

These hypothesis-driven schemes were captured by a DCM model space consisting of 11 models per phase (pre- or post-conditioning). Each model was estimated for each participant and each phase (pre- and post-conditioning) separately. Then, models were compared using a group-level random effects Bayesian Model Selection (BMS) approach (Stephan et al., 2009) to select the most probable model given the observed BOLD time-series. We employed a random effect approach (RFX BMS) to select the winning model, as

this method allows for the possibility that different participants may have different preferred models. The model exceedance probability (*p*_ex) used to find the best model as shown in **Figure 4B** represents the probability that a particular model is more likely than any other model in the model space, where the exceedance probabilities over the model space add to one.

Models shown in **Figure 4** assumed that high and low reward conditions are processed by the same brain regions and involve the same inter-areal connectivity patterns, albeit the strength of connections between areas were hypothesized to be modulated by reward. To test this latter hypothesis, we next inspected the winning model detected by RFX BMS approach and tested whether the connectivity strength of this model was modulated by reward magnitude using a Parametric Empirical Bayes (PEB) method (Zeidman et al., 2019). The PEB approach is a hierarchical Bayesian model that uses both non-linear (first-level) and linear (second-level) analyses. The advantage of this approach is that the inter-individual variability in model parameters is parameterized at the second level. Hence, parameter estimates for subjects with noisy data are likely to be adjusted in order to conform to the group distribution. Since our model comparison analysis revealed that model 10 had the strongest evidence in the post-conditioning (**Figure 4B**), we extracted the parameters of this model for both pre- and post-conditioning phases in each participant. These parameters provided the input to the first-level design matrix of the PEB. At the group level, the PEB included an additional binary regressor to model the difference between pre- and post-conditioning, as well as a constant term (i.e., mean parameter estimates across participants and conditioning phases). This allowed us to investigate how the connectivity strength was modulated by reward magnitude *after* participants had learned the reward-cue associations. As we were interested in the reward modulation of connections between regions, we focused on the estimated parameters in the modulatory (i.e., B matrix) connectivity for feedforward and feedback connections. Finally, for each connection, we report the reward modulation (high - low) posterior probabilities using a threshold of $P > 0.99$, correcting for multiple comparisons across connections (Bonferroni correction).

Results

We employed a visual discrimination task (VDT) during the test phase to examine the effects of the past reward associations learned during a reward conditioning task (**Figure 1**). The VDT task was tested before and after the reward conditioning task (referred to as the pre-

and post-conditioning, respectively). Our main findings concern the influence of the past reward cues from either the visual or auditory modality on the visual perception during the post-conditioning phase.

Conditioning phase: Recruitment of the classical brain regions involved in the reward associative learning

Participants exhibited near perfect accuracy in localizing both visual and auditory stimuli (both > 95%), however there was no significant effect of reward on either the response accuracies or the reaction times. Analysis of the BOLD responses revealed the classical brain areas that are involved in the associative learning of rewards, such as the ventral striatum and insula (see **Figure 2-1** and **Table 2-1** in the Extended Data). The effect of reward on the BOLD responses was largely independent of the sensory modality, except for the higher activations observed for the auditory compared to visual reward value found in the right caudate (**see Table 2-1** in the Extended Data).

Previously reward-associated cues slightly enhanced the speed of visual discrimination during the post-conditioning

We next examined the behavioural effects of rewards from the same (intra-modal) or different (cross-modal) sensory modality on the visual discrimination task. Compared to the pre-conditioning, reaction times decreased for all conditions during the post-conditioning phase indicating that with longer training on the task, participants' speed of perceptual decisions increased (**Table 1** and **Figure 2A**). This speed enhancement was stronger for the high compared to low reward conditions. Accordingly, we found a main effect of reward on the reaction times as higher reward magnitude increased the speed of visual discrimination across sensory modalities ($F(1,32) = 4.46$, $p = 0.04$, $\eta_p^2 = 0.12$). Other main and interaction effects did not reach statistical significance. The effect of reward in individual conditions (cross- and intra-modal conditions) was not significant (both ps>0.1), and although high reward stimuli seemed to lead to faster responses compared to the neutral condition, this effect did not reach statistical significance ($F(2,64) = 1.34$, $p = 0.268$, $\eta_p^2 = 0.040$). Analysis of the accuracies revealed neither a main effect of reward value nor an interaction with the sensory modality (both Fs<1.5 and ps>0.1). Together, these results indicate a weak behavioural advantage for high compared to low reward stimuli in our experiment which was mainly observed for the reaction times.

Reward-driven modulation of target representations in the early visual areas during the post-conditioning

We next examined how reward value affected the encoding of the target's tilt orientation in the early visual areas. To this end, we examined the results of the whole-brain searchlight *orientation decoder* (for classification of clockwise and counterclockwise orientations) and identified areas within an anatomical mask of area V1-V2 which exhibited a reward-driven increase in the decoding accuracy across sensory modalities in the post- compared to the pre-conditioning.

This contrast revealed a bilateral activation with a peak at xyz = [9 -64 5] in the right and at xyz = [-12 -67 2] in the left visual cortex (**Figure 2B**). Importantly, this activation overlapped with the regions within areas V1-V2 that were activated by the Gabor stimulus in the neutral condition indicating that they corresponded to the target-specific representations within the early visual areas (**Figure 2C**). This result indicates that higher reward enhanced the neural representation of the visual target already as early as in area V1-V2, in line with previous findings where reward-driven enhancement of the magnitude (Serences, 2008) or the specificity of spatial patterns (Pooresmaeili et al., 2014) of neural responses were observed in the early visual areas. Importantly, there was no statistically significant difference between the intra- and cross-modal reward-driven enhancement of target processing at the early visual areas as interaction contrasts revealed no activations even at very liberal thresholds (i.e., $p<0.01$, $k = 10$), indicating that the two types of rewards had similar impact on the processing of target in the early visual areas. Additionally, to further support these finding, we checked the opposite contrast (classification accuracy in Low Value > High Value) using the same threshold and mask and did not find any significant activation.

After establishing that higher reward enhances the reliability of target representations in the early visual areas, we asked *where* in the brain the associated reward value of stimuli is encoded and *how* the reward-related signals are communicated to the visual areas. In order to answer these questions, we conducted two types of analyses: 1) An MVPA analysis to identify *where* in the brain the reward value is encoded, and 2) An effective connectivity analysis in which the possible communication patterns between the identified valuation regions and early visual areas were tested (thus answering the question of *how*).

Identification of the brain regions that encode stimulus value during the post-conditioning (*where*)

Towards answering the first question regarding *where* in the brain the stimulus value is encoded after learning of the reward associations, we inspected the results of our two value decoders. To identify brain areas that are responsive exclusively to the stimulus reward magnitude irrespective of its sensory features (sensory modality and location), we inspected the results of the *value decoder 1* (see Material and Methods). This decoder performed a whole-brain search for regions that contained information about the reward value after value associations were learned (class labels were: high or low reward magnitude, see Material and Methods). The classification accuracy of *value decoder 1* was highest in a cluster in the left lateral orbitofrontal cortex (blue cluster in **Figure 3**, **Table 2,** and **Figure 3-1**), while several other areas related to the reward processing such as ventral striatum, ventromedial prefrontal cortex were also identified by this analysis (**Table 2**). The lateral OFC cluster was further selected for the subsequent effective connectivity analysis.

Next, we asked which brain areas are involved in the encoding of stimulus value specifically for each sensory modality and stimulus location. These areas are instrumental in conveying additional information regarding the specific sensory feature of reward cues across the brain. In order to investigate this question, we examined the results of the *value decoder 2* which decoded the stimulus value separately for each sensory modality (intra- and cross-modal) and stimulus location (left and right, see the Material and Methods). We then inspected the results of this decoder across both sensory modalities as well as differentially contrasting one modality against the other. The strongest reward modulation across sensory modalities was observed in the superior temporal areas (STS, red cluster in **Figure 3,** see also **Figure 3-1**), an area that is tightly linked to multisensory processing (Calvert et al., 2001; Stein and Stanford, 2008). Interestingly, we also found that across sensory modalities, stimulus value was reliably decoded from regions with a known role in attentional processing such as a large cluster in the anterior intraparietal area (IPS, green cluster in **Figure 3,** see also **Figure 3-1**). This area has not only been related to the attentional selection (Corbetta and Shulman, 2002), but also has been shown to be modulated by reward (Platt and Glimcher, 1999; Bendiksby and Platt, 2006; Louie et al., 2011). Moreover, we also observed several areas such as the cuneus, cingulate, temporoparietal area, and motor cortex which contained reliable representations of stimulus value across modalities (see **Table 2**).

To test whether there are specific brain areas that contain more information about the stimulus value from one compared to another sensory modality, we contrasted the whole-brain results of the *value decoder 2* for Auditory (Cross-modal) >Visual (intra-modal) and vice versa. The first contrast (i.e., classification accuracy in auditory > classification accuracy in visual), revealed a cluster in the left auditory cortex which corresponded to the primary auditory cortex (area A1, at $p < 0.005$, k = 20 uncorrected). However, in the intra-modal interaction (i.e. classification accuracy in visual > classification accuracy in auditory), no voxel survived at the same threshold (at $p < 0.005$, k =20 uncorrected, see **Table 2**).

Based on the above results and our a priori hypotheses, we took the IPS and STS clusters as ROIs that might be involved in the long-range communications between the valuation network (i.e., OFC, identified by *value decoder 1*) and the early visual areas (i.e, EVA, identified by the *orientation decoder*), as they were discriminative of reward value across sensory modalities. Furthermore, *value decoder 2* only identified the primary auditory cortex (area A1) as an area that contained more information about one over the other sensory modality (cross-modal > intra-modal), whereas we did not find any area that selectively encoded the value of intra-modal stimuli. In contrast to the A1, that might play a role in processing the sensory features of the auditory reward-associated cues, the superior temporal areas are known to be involved in higher-order auditory processing and the integration of information across senses (Stein and Stanford, 2008), where most likely both the visual target and auditory reward-associated cues were processed. In fact, when we inspected the results of *value decoder 2* in each individual modality, we observed STS activations for both intra- and cross-modal value (**Table 2**). We therefore reasoned that including STS but not A1 in our effective connectivity analyses would capture the reward-driven effects of both cross-modal and intra-modal stimuli, while reducing the complexity of models by adding multiple areas with overlapping functionalities (i.e., STS and A1).

Effective connectivity analysis revealed *how* reward information is broadcasted across the brain

After identifying the potential brain areas that mediate the reward-driven modulation of early visual areas, we tested possible models of *how* reward information is broadcasted across the brain using an effective connectivity approach. Based on our hypotheses, three possibilities existed which gave rise to 11 biologically plausible schemes in our model space (**Figure 4A**): **1)** reward signals are communicated indifferently from the reward-related areas to the early visual areas, involving either a long-range direct projection (**fig.4A**, model 1) or

606 mediation through the attention-related or higher sensory-related areas (**fig.4A**, model 2-4), **2)**
607 reward signals are communicated following a modality-specific pathway through attention
608 and/or higher sensory-related areas (**fig.4A**, model 5-10), or **3)** reward signals have a long-
609 lasting effect where the neural plasticity in the early visual areas is altered locally without the
610 necessity of information flow from and to the other brain areas (**fig.4A**, model 11 or *null*, see
611 the Material and Methods). These models thus differed with respect to the nodes/regions and
612 connectivity patterns which underlay the intra-modal and cross-modal information transfer.
613 In all models, high and low reward conditions involved the same nodes and connectivity
614 patterns but could influence the strength of the connectivity between each pair of nodes to a
615 different extent (see Material and Methods). Therefore, we first established which nodes and
616 connectivity patterns best explained the BOLD times series of the intra- and cross-modal
617 conditions in pre- and post-conditioning and thereafter tested whether the strength of
618 connections in the winning model was modulated by reward magnitude after the stimulus-
619 reward associations were learned.

620 Among the possible models, our results (**Figure 4B**) indicated that model 10 gained
621 the highest evidence in the post-conditioning ($p\_ex = 0.42$) relative to the second best model
622 (model 4, $p\_ex = 0.2$). Meanwhile, model *null* gained the highest evidence in the pre-
623 conditioning ($p\_ex = 0.99$). As expected, learning of the reward associations changed the way
624 that information was communicated across the brain, as reward-related areas were only
625 involved in modulating the early visual areas *after* the stimulus-reward associations had been
626 established. In the winning model 10 in the post-conditioning, intra- and cross-modal
627 information needed to be gated through the regions involved in the attentional selection, as
628 IPS was involved in mediating both communication paths. Additionally, the cross-modal
629 condition engaged the STS, a higher-order sensory area, in order to communicate the reward
630 information across the brain. This is aligned with our hypothesis 2, where intra- and cross-
631 modal effects were mediated through both attention and sensory-dependent areas.

632 In order to infer how reward value modulated the strength of connectivity between
633 every pair of nodes/regions in the winning model, we next conducted a group level analysis
634 on the weights of feedforward and feedback connections. We included both pre- and post-
635 conditioning data of the winning model (model 10 in the post-conditioning) in our design
636 matrix and examined the reward-driven changes in the weights of connections that occurred
637 after the stimulus-reward associations were learned by regressing out the effects in the pre-
638 conditioning (see the Material and Methods). This analysis summarised in **Figure 4C**,

revealed widespread effects of reward value on the strength of connections between different regions. Specifically, we found both modality-independent and modality-dependent reward modulations. The feedback connectivity from the valuation area (OFC) to the mediation areas in IPS for both intra- and cross-modal and further between IPS and STS in cross-modal condition were predominantly inhibitory (OFC-IPS: -0.47 Hz and -0.34 Hz in intra- and cross-modal, respectively, with no significant difference between the two: posterior probability $P = 0.88$; and IPS-STS in cross-modal: -0.53Hz), likely to prevent the allocation of processing resources to high reward cues that were irrelevant to the target discrimination. However, there was a dissociation in the feedforward communication paths (i.e., modality-dependent), where intra-modal cues relied on an excitatory modulation (IPS-OFC: 0.09 Hz) and cross-modal cues relied on inhibitory modulations (IPS-OFC: -0.22 Hz and STS-IPS: -0.21 Hz), with a significant difference between the two modalities at the level of IPS-OFC involved in processing of both cross- and intra-modal conditions (posterior probability $P > 0.99$). The dissociation between intra- and cross-modal feedforward connections might indicate that mediation areas (IPS and STS) engage distinct mechanisms to prioritize the processing of sensory features of the high reward stimuli. Specifically, feedforward processing of intra-modal rewards was enhanced due to the need to discriminate the intra-modal reward cues from the visual target as both emanated from the same sensory modality, whereas the feedforward processing of cross-modal reward cues that were distinct from the visual target decreased. Remarkably, the dissociation of reward effects was further enhanced while examining the connections to and from the early visual areas (EVA). At this level, intra-modal cues relied more on the inhibitory and cross-modal cues on the excitatory feedback modulations. Specifically, whereas the feedback communication in the intra-modal condition was suppressed (IPS-EVA: -0.23 Hz), both feedback (STS-EVA: 0.33 Hz) and feedforward (EVA-STS: 0.46 Hz) communication paths were facilitated for cross-modal cues. This distinction might indicate that the way higher reward increases the perceptual discriminability of the target may differ between the intra- and cross-modal conditions, where intra-modal rewards boost the differentiation and cross-modal rewards increase the integration of the reward cues and the target. Accordingly, the top-down inhibitory modulation from the IPS to EVA likely suppresses the processing of the high reward intra-modal cues (i.e., irrelevant information) to improve the representation of the target. In contrast, enhancing the feedforward processing of the visual target in EVA-STS, could potentially enhance the integration of the auditory reward-associated cues and the visual

672 target and subsequently the excitatory feedback from the STS to EVA could boost the
673 representation of the target.

674 Discussion

675 This study aimed to investigate the reward-driven modulation of the early visual
676 processing. We compared intra- and cross-modal previously reward associated cues to probe
677 whether their reward-driven effects depended on the sensory modality of the cues. In our
678 paradigm using a visual discrimination task, previously reward associated task-irrelevant cues
679 slightly improved the speed of perceptual decisions. Moreover, using a multivariate pattern
680 classification approach, we observed that high reward stimuli enhanced the neural
681 representations of the target in the early visual areas. We looked further into the possible
682 neural mechanisms governing this effect by means of an effective connectivity analysis. This
683 analysis revealed that reward-related information is communicated across the brain in both
684 modality-independent and modality-dependent manners. In general, the reward-driven effects
685 of both intra- and cross-modal cues recruited areas involved in the encoding of reward value
686 and attentional selection. However, cross-modal rewards additionally involved the higher-
687 order sensory-related areas such as STS. The feedback communication between these areas
688 was predominantly inhibitory, suggesting that reward value may modulate the prioritization
689 of information processing. Unlike the modality-independent interactions observed between
690 the higher-level areas, the neural communication to and from the early visual areas were
691 differentially modulated by intra- and cross-modal rewards. At this level, intra-modal rewards
692 produced predominantly feedback inhibition whereas cross-modal rewards led to excitatory
693 feedforward and feedback modulations.

694 Previously reward associated cues have been known to capture attention (Anderson et
695 al., 2011). Consequently, when reward cues are not the target of the task, response times are
696 slowed down as attention needs to be re-oriented from the reward-associated task-irrelevant
697 distractors to the target. In our study, we observed a weak facilitation (i.e., faster reaction
698 times) by the irrelevant high reward cues. A possible reason is the spatial alignment of the
699 reward cues and target in our study that differed from Anderson and colleagues (Anderson et
700 al., 2011), where in their design, reward cues and target were separated spatially. In contrast,
701 in our design reward cues and the visual target were presented at the same location.
702 Therefore, attention did not need to be re-oriented and the capture of attention created by the
703 irrelevant reward cues could potentially spill over to the target, energizing the responses.

Moreover, in contrast to our previous study (Vakhrushev et al., 2023), where perceptual discrimination and visual event-related potentials were either suppressed or enhanced by the intra- and cross-modal rewards, respectively, we did not observe an interaction effect. An aspect that differed with this previous study was the length of training on the task before the reward associations were learned, where in the current study the number of trials in the pre-conditioning phase was doubled so that participants are better accustomed to the reward cues and their relation to the task. This extended training might have allowed that the competition between the target and the task-irrelevant cues, especially those from the same sensory modality, is better resolved. In fact, in a subsequent study (Antono et al., 2022), we showed that after being exposed to the intra- and cross-modal reward cues that were predictive of the delivery of the reward upon correct performance, the visual discrimination was enhanced by previously rewarded cues of both modalities. This finding supports the idea that the duration of training and the history of reward delivery may influence the way that task-irrelevant previously rewarded stimuli affect the perceptual decisions (Jahfari and Theeuwes, 2017; Jahfari et al., 2020). Future studies will be needed to systematically investigate these factors.

In line with the behavioural results, we found that early visual areas within the anatomical boundaries of area V1 – V2 had a better representation of the tilt orientation of the target when the target was presented together with the high reward stimuli. Reward signals have been known to modulate the early sensory areas (*visual*: Bayer et al., 2017; Serences, 2008, *auditory*: Beitel, et al., 2003; Guo, et al., 2019, *somatosensory*: Pleger, et al., 2008). More specifically, it has been known that the early visual areas are sensitive to the reward magnitude (Serences, 2008; Weil et al., 2010; Arsenault et al., 2013) and timing (Shuler & Bear, 2006; Chubykin, et al., 2013). Importantly, the reward-driven modulations in our study were spatially specific and overlapped with the regions within the area V1-V2 that represented the visual target, in line with previous observations (Serences, 2008; Arsenault et al., 2013). In contrast, other studies have provided evidence that reward effects may rely on a combination of stimulus-specific and unspecific modulations, suggesting that reward learning in the visual system may be gated by mechanisms that are distinct from sensory processing (FitzGerald et al., 2013; Schiffer et al., 2014; Poort et al., 2015). Since in our design we did not manipulate the spatial location of stimuli and the delivery of rewards was halted during the test phase, we cannot infer the extent to which the spatial profile of reward-driven effects in our study reflects a general principle as opposed to a particular pattern imposed by our task

736 design. Unravelling the spatial characteristics of reward-driven modulations from different
737 sensory modalities is an important direction for future studies.

738 What mechanisms underlie the reward-driven enhancement of target representations
739 in the early visual areas? We sought the answer to this question by first mapping the areas
740 where the reward value was represented and thereafter testing different models of how
741 reward information could be communicated between the valuation and early visual areas.
742 Using a multivariate pattern classification approach, the lateral orbitofrontal cortex (OFC)
743 was identified as a region that reliably encoded stimulus value independent of the sensory
744 features of the reward associated stimuli. Previous studies have shown that this area plays a
745 key role in representing the magnitude of rewards, especially when there is uncertainty in the
746 appropriate course of action to be taken such as when previously rewarded responses should
747 be suppressed (Elliott et al., 2000; J. et al., 2001). Furthermore, IPS and STS were identified
748 by the value decoders which were sensitive to the sensory features of the reward stimuli (i.e.,
749 modality and location). IPS has been consistently linked to the processing of the goal-directed
750 information and voluntary orienting towards a spatial location (Corbetta et al., 2000; Corbetta
751 and Shulman, 2002; Serences and Yantis, 2007), within and across sensory modalities (Lewis
752 et al., 2000; Saito et al., 2005). The involvement of IPS in representing the reward value is in
753 line with the previous reports of similar effects in the visual domain (Platt and Glimcher,
754 1999; Bendiksby and Platt, 2006; Louie et al., 2011) and supports the notion of a general role
755 of this region in the top-down modulation of visual processing that could also be elicited
756 cross-modally (Eimer and Driver, 2001; Hillyard et al., 2016). Specifically, the coordinates
757 observed in our study is close to the anterior part of the IPS with dense neuroanatomical
758 connectivity with the frontal areas (Greenberg et al., 2012), suggesting that the modulation of
759 IPS may be driven by the top-down signals from the frontal valuation areas. The superior
760 temporal areas such as STS have been classically shown to be involved in the integration of
761 information across sensory modalities (Calvert et al., 2001; Werner and Noppeney, 2010).
762 Moreover, the role of this area in the integration of information has been shown to go beyond
763 the multisensory processing and also include a general role in linking the sensory attributes of
764 stimuli to the cognitive factors such as attention (Shapiro and Hillstrom, 2002), reward (Lim
765 et al., 2013; Pooresmaeili et al., 2014) and affective and social processing (Beauchamp,
766 2015). Importantly, STS and IPS have been shown to have structural connectivity (Cavada
767 and Goldman-Rakic, 1989) and form a network for attentional (Shapiro and Hillstrom, 2002)
768 and multisensory processing (Werner and Noppeney, 2010), and additionally STS has been

shown to communicate the reward-related information to the frontal valuation areas (Lim et al., 2013). Given these findings from the previous studies, the valuation areas identified by our approach constituted a plausible network, shown in **Figure 4,** to represent and communicate the information related to the reward value across the brain.

We next used an effective connectivity analysis to explicitly test how such a putative communication occurs. We tested different mechanisms that either relied on a direct or a mediated communication between the valuation and the early visual areas. This analysis supported a model which assumed the mediation of reward effects through attention and/or higher sensory areas. The communication between the valuation- and attention-related areas are aligned with the notion of attentional gated reward processing (Roelfsema and Van Ooyen, 2005). In line with this model, we found that when there was a need to discriminate the sensory features of reward- and task-related stimuli, as was the case when reward cues were from the same modality, the feedforward communication between the attentional and the valuation network was enhanced relative to when reward-related stimuli were highly distinct from the visual target (i.e., for cross-modal cues). On the other hand, previous studies have also proposed rewards to be a teaching signal for attention (Chelazzi et al., 2013), as the magnitude of reward determines the way that attention should be allocated in space. In line with this proposal, we found a general pattern across the sensory modalities where higher areas sent inhibitory feedback signals to upstream attentional and higher-order sensory areas, potentially in order to suppress the excessive allocation of attention and other processing resources to the task-irrelevant cues. Together, our findings from a model-based approach that we took in this study provide preliminary hints towards the fine-tuned mechanisms that underlie the regulation of attention and reward processing across the sensory modalities, which await further corroboration from the future studies.

The pattern of connectivity modulations at the lower levels of the network shown in **Figure 4C** revealed further dissociations between the intra- and cross-modal rewards. Specifically, the communication from the IPS back to the early visual areas demonstrated a distinct pattern across intra- and cross-modal conditions. Whereas reward-related information was communicated from IPS directly to the early visual areas and elicited feedback inhibition, cross-modal cues required a mediation through a sensory-dependent area in the superior temporal areas and modulated the early visual areas through excitatory interactions. This pattern is in line with the findings of a previous study (Vakhrushev et al., 2023) where a dissociation between the reward-driven effects of previously rewarded intra- and cross-modal

802 cues was found. Putatively, the feedback inhibition in case of the intra-modal reward cues
803 reflects the down-weighting of the value of the task-irrelevant features of an object (i.e., the
804 colors), which share processing resources with the target. In fact, recent studies have shown
805 that at the level of area V1, processing of orientation and color is more inter-related than
806 previously thought (Garg et al., 2019). This means that by regulating the processing of high
807 reward colors through feedback inhibition, the early visual areas could better dedicate
808 resources to the representation of the stimulus orientation, a proposal that is in line with a
809 host of previous studies on the value-driven capture of attention by high reward visual
810 distractors (Hickey et al., 2010; Anderson et al., 2011; Itthipuripat et al., 2019; Adam and
811 Serences, 2021). In contrast, in the cross-modal condition, there is little necessity to suppress
812 the reward cues as they elicit a relatively weaker competition with the target at the level of
813 the early visual areas. In fact, through enhancing the allocation of attention (Eimer and
814 Driver, 2001; Hillyard et al., 2016) or the integration of the auditory tones and visual stimuli
815 (Driver and Noesselt, 2008; Petro et al., 2017), a boost in the processing of cross-modal
816 reward cues could potentially enhance the overall salience of the visual target at the level of
817 early visual areas.

818 Altogether, the commonalities and dissociations between intra- and cross-modal
819 rewards observed in the effective connectivity results point to two general patterns. Firstly,
820 both reward types engage attentional areas and lead to a predominantly inhibitory feedback
821 connectivity between the valuation and attentional areas. Hence, the regulation of information
822 processing at the level of higher cognition seems to be modality-independent. Secondly, at
823 the lower levels of hierarchy where reward-related information is relayed to the early visual
824 areas, more dissociations between the intra- and cross-modal rewards emerge: not only do the
825 cross-modal rewards additionally engage a higher-order sensory area (STS) but also, they
826 elicit an overall enhanced communication to and from the early visual areas, whereas intra-
827 modal rewards evoked an overall inhibition. We interpret the dissociations between the intra-
828 and cross-modal reward effects as a consequence of the differences in the way that they
829 interact with the processing of the target at the level of early visual areas, with visual reward
830 cues interfering with the processing of the target more strongly that the auditory reward cues.
831 Future studies will be needed to test whether a systematic relationship exists between the
832 degree of overlap in neural mechanisms of task-relevant and reward-related features of
833 stimuli and the way that perceptual decisions are influenced by the rewards.

Using a DCM approach (Friston et al., 2003) to model effective connectivity was well-suited for the purpose of our study since it enabled us to test a set of pre-specified generative models in terms of their fit to the fMRI time series. However, we note that this method has important biophysical (for instance the extent to which the approximation of neurovascular coupling can capture the task-related changes in the neural states) and statistical (the complexity of model parameters and generalizability) limitations (Daunizeau et al., 2011). In fact, rather than providing a "true" picture of the mechanisms through which the inter-regional neural interactions occur, DCM aims to infer the most plausible interactions among hidden neural states that cause the task-induced fluctuations of fMRI time series (Stephan et al., 2010). Given these considerations, the findings of our study provide preliminary hints towards mechanisms that underlie reward-driven effects on sensory perception and await validation by more fine-grained methods, such as multi-regional recordings in animals (for the application of DCM to neurophysiological data see Bastos et al., 2012; Mejias et al., 2023) or multi-modal imaging techniques (e.g. concurrent EEG-fMRI as done in David et al., 2008).

Previous theoretical and empirical work has suggested a tight interaction between reward and attention (Roelfsema and Van Ooyen, 2005; Stanisor et al., 2013). In this vein, it has been suggested that attention and reward reinforcement (Seitz and Watanabe, 2009) can work as heuristics which help the visual system to determine the sensory features that are relevant. Similarly, Padmala and Pessoa (2011) discussed that reward information enables a coupling between the attentional and valuation networks. Specifically, comparing the functional connectivity of rewarded and not-rewarded trials (Padmala and Pessoa, 2011; Kinnison et al., 2012) they found that whereas in rewarded trials attentional and valuation mechanisms worked as an integrated system, in not-rewarded trials they worked more independently from each other. Extending these findings, we showed that the coordination of attention and valuation may additionally occur for previously rewarded stimuli and engage higher-order sensory areas such as STS. An important direction for future studies will be to examine whether the mode of interaction between reward-, attention- and sensory-related areas holds under different contexts for instance different attentional loads and contingencies of rewards to performance (Antono et al., 2022). Our hypothesis is that the visual system will engage both attention and reward systems as resources to learn and change its plasticity. However, depending on the availability and the reliability of the resources, it can flexibly rely on one system rather than the other. Furthermore, future studies will be needed to delineate

whether the involvement of the long-range interactions to and from the sensory areas is a general feature of reward-driven modulation of perception or a specific finding in the setting that we tested. It is conceivable that when rewards are consistently paired with the task-relevant features, they may induce long-lasting changes at the level of early sensory areas that locally enhance the processing of reward-related stimuli, as predicted by computational models (Wilmes and Clopath, 2019). In these cases, a long-term prioritization of reward-related stimuli is advantageous for the system as they could consistently lead to a behavioural gain for the organism. Quantifying the exact relationship between rewards' availability and reliability and the degree to which they promote long-term plasticity in the early sensory areas is an exciting direction for future studies.

Acknowledgements

We thank Tabea Hildebrand, Jana Znaniewitz, and Sanna Peter for their help with the data collection. We also thank Dr. Carsten Schmidt-Samoa and Dr. Peter Dechent for their technical assistance, and Prof. Melanie Wilke and Dr. Roberto Goya-Maldonado for their input and suggestions. This work was supported by an ERC Starting Grant (no: 716846) to AP.

Authors' contributions

JEA and AP conceptualized the project designed the task. JEA conducted the experiments. JEA, SD, RA, and AP analyzed the data. JEA and AP interpreted the results and wrote the first draft of the manuscript. All authors revised the manuscript. AP acquired funding.

References

Adam KCS, Serences JT (2021) History modulates early sensory processing of salient distractors. J Neurosci 41:8007–8022.

Algazi VR, Duda RO, Thompson DM, Avendano C (2001) The CIPIC HRTF database. IEEE ASSP Work Appl Signal Process to Audio Acoust:99–102.

Anderson BA (2017) Reward processing in the value-driven attention network: Reward signals tracking cue identity and location. Soc Cogn Affect Neurosci 12:461–467.

Anderson BA, Laurent PA, Yantis S (2011) Value-driven attentional capture. Proc Natl Acad Sci U S A 108:10367–10371.

Antono JE, Vakhrushev R, Pooresmaeili A (2022) Value-driven modulation of visual perception by visual and auditory reward cues: The role of performance-contingent delivery of reward. Front Hum Neurosci 16.

Arsenault JT, Nelissen K, Jarraya B, Vanduffel W (2013) Dopaminergic Reward Signals Selectively Decrease fMRI Activity in Primate Visual Cortex. Neuron 77:1174–1186.

Barbas H (1993) Organization of cortical afferent input to orbitofrontal areas in the rhesus monkey.

Neuroscience 56:841–864.

Bastos AM, Usrey WM, Adams RA, Mangun GR, Fries P, Friston KJ (2012) Canonical microcircuits for predictive coding. Neuron 76:695–711.

Bayer M, Rossi V, Vanlessen N, Grass A, Schacht A, Pourtois G (2017) Independent effects of motivation and spatial attention in the human visual cortex. Soc Cogn Affect Neurosci 12:146–156.

Beauchamp MS (2015) The social mysteries of the superior temporal sulcus. Trends Cogn Sci 19:489–490.

Beitel RE, Schreiner CE, Cheung SW, Wang X, Merzenich MM (2003) Reward-dependent plasticity in the primary auditory cortex of adult monkeys trained to discriminate temporally modulated signals. Proc Natl Acad Sci U S A 100:11070–11075.

Bendiksby MS, Platt ML (2006) Neural correlates of reward and attention in macaque area LIP. Neuropsychologia 44:2411–2420.

Bray S, Arnold AEGF, Iaria G, MacQueen G (2013) Structural connectivity of visuotopic intraparietal sulcus. Neuroimage 82:137–145.

Calvert GA, Campbell R, Brammer MJ (2000) Evidence from functional magnetic resonance imaging of crossmodal binding in the human heteromodal cortex. Curr Biol 10:649–657.

Calvert GA, Hansen PC, Iversen SD, Brammer MJ (2001) Detection of audio-visual integration sites in humans by application of electrophysiological criteria to the BOLD effect. Neuroimage 14:427–438.

Carmichael ST, Price JL (1995) Sensory and premotor connections of the orbital and medial prefrontal cortex of macaque monkeys. J Comp Neurol 363:642–664.

Cavada C, Goldman-Rakic PS (1989) Posterior parietal cortex in rhesus monkey: I. Parcellation of areas based on distinctive limbic and sensory corticocortical connections. J Comp Neurol 287:393–421.

Chelazzi L, Perlato A, Santandrea E, Della Libera C (2013) Rewards teach visual selective attention. Vision Res 85:58–72.

Cheng FPH, Saglam A, André S, Pooresmaeili A (2020) Cross-modal integration of reward value during oculomotor planning. eNeuro 7.

Chubykin AA, Roach EB, Bear MF, Shuler MGH (2013) A Cholinergic Mechanism for Reward Timing within Primary Visual Cortex. Neuron 77:723–735.

Cicmil N, Cumming BG, Parker AJ, Krug K (2015) Reward modulates the effect of visual cortical microstimulation on perceptual decisions. Elife 4:1–25.

Corbetta M, Kincade JM, Ollinger JM, McAvoy MP, Shulman GL (2000) Erratum: Voluntary orienting is dissociated from target detection in human posterior parietal cortex (Nature Neuroscience (2000) 3 (292-297)). Nat Neurosci 3:521.

Corbetta M, Shulman GL (2002) Control of goal-directed and stimulus-driven attention in the brain. Nat Rev Neurosci 3:201–215.

Daniel R, Pollmann S (2014) A universal role of the ventral striatum in reward-based learning: evidence from human studies. Neurobiol Learn Mem 114:90–100.

Daunizeau J, David O, Stephan KE (2011) Dynamic causal modelling: a critical review of the biophysical and statistical foundations. Neuroimage 58:312–322.

David O, Guillemain I, Saillet S, Reyt S, Deransart C, Segebarth C, Depaulis A (2008) Identifying Neural Drivers with Functional MRI: An Electrophysiological Validation. PLOS Biol 6:e315.

Driver J, Noesselt T (2008) Multisensory Interplay Reveals Crossmodal Influences on "Sensory-Specific" Brain Regions, Neural Responses, and Judgments. Neuron 57:11–23.

Eickhoff SB, Stephan KE, Mohlberg H, Grefkes C, Fink GR, Amunts K, Zilles K (2005) A new SPM toolbox for combining probabilistic cytoarchitectonic maps and functional imaging data. Neuroimage 25:1325–1335.

946 Eimer M, Driver J (2001) Crossmodal links in endogenous and exogenous spatial attention: Evidence from
947 event-related brain potential studies. In: Neuroscience and Biobehavioral Reviews, pp 497–511. Neurosci
948 Biobehav Rev.

949 Elliott R, Friston KJ, Dolan RJ (2000) Dissociable neural responses in human reward systems. J Neurosci
950 20:6159–6165.

951 Felleman DJ, Van Essen DC (1991) Distributed hierarchical processing in the primate cerebral cortex. Cereb
952 Cortex 1:1–47.

953 FitzGerald THB, Friston KJ, Dolan RJ (2013) Characterising reward outcome signals in sensory cortex.
954 Neuroimage 83:329–334.

955 Friston KJ, Harrison L, Penny W (2003) Dynamic causal modelling. Neuroimage 19:1273–1302.

956 Garg AK, Li P, Rashid MS, Callaway EM (2019) Color and orientation are jointly coded and spatially organized
957 in primate primary visual cortex. Science (80-) 364:1275–1279.

958 Gluth S, Rieskamp J, Büchel C (2014) Neural evidence for adaptive strategy selection in value-based decision-
959 making. Cereb Cortex 24:2009–2021.

960 Goltstein PM, Coffey EBJ, Roelfsema PR, Pennartz CMA (2013) In vivo two-photon Ca2+ imaging reveals
961 selective reward effects on stimulus-specific assemblies in mouse visual cortex. J Neurosci 33:11540–
962 11555.

963 Gong M, Jia K, Li S (2017) Perceptual competition promotes suppression of reward salience in behavioral
964 selection and neural representation. J Neurosci 37:6242–6252.

965 Greenberg AS, Verstynen T, Chiu YC, Yantis S, Schneider W, Behrmann M (2012) Visuotopic cortical
966 connectivity underlying attention revealed with white-matter tractography. J Neurosci 32:2773–2782.

967 Grill-Spector K (2003) The neural basis of object perception. Curr Opin Neurobiol 13:159–166.

968 Grill-Spector K, Malach R (2004) The human visual cortex. Annu Rev Neurosci 27:649–677.

969 Guo L, Weems JT, Walker WI, Levichev A, Jaramillo S (2019) Choice-selective neurons in the auditory cortex
970 and in its striatal target encode reward expectation. J Neurosci 39:3687–3697.

971 Haber SN (2011) Neuroanatomy of Reward: A View from the Ventral Striatum. CRC Press/Taylor & Francis.

972 Haber SN, Knutson B (2010) The reward circuit: Linking primate anatomy and human imaging.
973 Neuropsychopharmacology 35:4–26.

974 Hickey C, Chelazzi L, Theeuwes J (2010) Reward changes salience in human vision via the anterior cingulate. J
975 Neurosci 30:11096–11103.

976 Hillyard SA, Störmer VS, Feng W, Martinez A, McDonald JJ (2016) Cross-modal orienting of visual attention.
977 Neuropsychologia 83:170–178.

978 Hubel DH, Wiesel TN (1968) Receptive fields and functional architecture of monkey striate cortex. J Physiol
979 195:215–243.

980 Itthipuripat S, Vo VA, Sprague TC, Serences JT (2019) Value-driven attentional capture enhances distractor
981 representations in early visual cortex. PLoS Biol 17:e3000186.

982 J. O, M.L. K, E.T. R, J. H, C. A, O'Doherty J, Kringelbach ML, Rolls ET, Hornak J, Andrews C (2001)
983 Abstract reward and punishment representations in the human orbitofrontal cortex. 4:95–102.

984 Jacob SN, Nienborg H (2018) Monoaminergic Neuromodulation of Sensory Processing. Front Neural Circuits
985 12:51.

986 Jahfari S, Theeuwes J (2017) Sensitivity to value-driven attention is predicted by how we learn from value.
987 Psychon Bull Rev 24:408–415.

988 Jahfari S, Theeuwes J, Knapen T (2020) Learning in Visual Regions as Support for the Bias in Future Value-
989 Driven Choice. Cereb Cortex 30:2005–2018.

990 Khibnik LA, Tritsch NX, Sabatini BL (2014) A direct projection from mouse primary visual cortex to
991 dorsomedial striatum. PLoS One 9.

992 Kim H, Anderson BA (2019) Dissociable neural mechanisms underlie value-driven and selection-driven
993 attentional capture. Brain Res 1708:109–115.

994 Kinnison J, Padmala S, Choi JM, Pessoa L (2012) Network analysis reveals increased integration during
995 emotional and motivational processing. J Neurosci 32:8361–8372.

996 Komura Y, Tamura R, Uwano T, Nishijo H, Kaga K, Ono T (2001) Retrospective and prospective coding for
997 predicted reward in the sensory thalamus. Nature 412:546–549.

998 Kourtzi Z, Kanwisher N (2001) Representation of perceived object shape by the human lateral occipital
999 complex. Science (80-) 293:1506–1509.

1000 Kringelbach ML (2005) The human orbitofrontal cortex: linking reward to hedonic experience. Nat Rev
1001 Neurosci 6:691–702.

1002 Kveraga K, Boshyan J, Bar M (2007) Magnocellular projections as the trigger of top-down facilitation in
1003 recognition. J Neurosci 27:13232–13240.

1004 Lewis JW, Beauchamp MS, DeYoe EA (2000) A Comparison of Visual and Auditory Motion Processing in
1005 Human Cerebral Cortex. Cereb Cortex 10:873–888.

1006 Lewis R, Noppeney U (2010) Audiovisual synchrony improves motion discrimination via enhanced
1007 connectivity between early visual and auditory areas. J Neurosci 30:12329–12339.

1008 Lim SL, O'Doherty JP, Rangel A (2013) Stimulus value signals in ventromedial PFC reflect the integration of
1009 attribute value signals computed in fusiform gyrus and posterior superior temporal gyrus. J Neurosci
1010 33:8729–8741.

1011 Lingnau A, Strnad L, He C, Fabbri S, Han Z, Bi Y, Caramazza A (2014) Cross-modal plasticity preserves
1012 functional specialization in posterior parietal cortex. Cereb Cortex 24:541–549.

1013 Louie K, Grattan LE, Glimcher PW (2011) Reward value-based gain control: Divisive normalization in parietal
1014 cortex. J Neurosci 31:10627–10639.

1015 Macedo-Lima M, Remage-Healey L (2021) Dopamine Modulation of Motor and Sensory Cortical Plasticity
1016 among Vertebrates. In: Integrative and Comparative Biology, pp 316–336. Oxford University Press.

1017 Martin CB, Douglas D, Newsome RN, Man LLY, Barense MD (2018) Integrative and distinctive coding of
1018 visual and conceptual object features in the ventral visual stream. Elife 7.

1019 Mejias JF, Murray JD, Kennedy H, Wang X-J (2023) Feedforward and feedback frequency-dependent
1020 interactions in a large-scale laminar network of the primate cortex. Sci Adv 2:e1601335.

1021 Noesselt T, Rieger JW, Schoenfeld MA, Kanowski M, Hinrichs H, Heinze HJ, Driver J (2007) Audiovisual
1022 temporal correspondence modulates human multisensory superior temporal sulcus plus primary sensory
1023 cortices. J Neurosci 27:11431–11441.

1024 Noudoost B, Moore T (2011) Control of visual cortical signals by prefrontal dopamine. Nature 474:372–375.

1025 Oades RD, Halliday GM (1987) Ventral tegmental (A10) system: neurobiology. 1. Anatomy and connectivity.
1026 Brain Res Rev 12:117–165.

1027 Padmala S, Pessoa L (2011) Reward reduces conflict by enhancing attentional control and biasing visual cortical
1028 processing. J Cogn Neurosci 23:3419–3432.

1029 Pessoa L (2009) How do emotion and motivation direct executive control? Trends Cogn Sci 13:160–166.

1030 Pessoa L (2015) Multiple influences of reward on perception and attention. Vis cogn 23:272–290.

1031 Pessoa L, Engelmann JB (2010) Embedding reward signals into perception and cognition. Frontiers Media SA.

1032 Petro LS, Paton AT, Muckli L (2017) Contextual modulation of primary visual cortex by auditory signals.
1033 Philos Trans R Soc B Biol Sci 372:20160104.

1034 Platt ML, Glimcher PW (1999) Neural correlates of decision variables in parietal cortex. Nature 400:233–238.

1035 Pleger B, Blankenburg F, Ruff CC, Driver J, Dolan RJ (2008) Reward facilitates tactile judgments and
1036 modulates hemodynamic responses in human primary somatosensory cortex. J Neurosci 28:8161–8168.

1037 Pooresmaeili A, FitzGerald THB, Bach DR, Toelch U, Ostendorf F, Dolan RJ (2014) Cross-modal effects of
1038 value on perceptual acuity and stimulus encoding. Proc Natl Acad Sci U S A 111:15244–15249.

1039 Poort J, Khan AG, Pachitariu M, Nemri A, Orsolic I, Krupic J, Bauza M, Sahani M, Keller GB, Mrsic-Flogel
1040 TD, Hofer SB (2015) Learning Enhances Sensory and Multiple Non-sensory Representations in Primary
1041 Visual Cortex. Neuron 86:1478–1490.

1042 Rangel A, Camerer C, Montague PR (2008) A framework for studying the neurobiology of value-based decision
1043 making. Nat Rev Neurosci 9:545–556.

1044 Reig R, Silberberg G (2014) Multisensory Integration in the Mouse Striatum. Neuron 83:1200–1212.

1045 Roelfsema PR, Van Ooyen A (2005) Attention-gated reinforcement learning of internal representations for
1046 classification. Neural Comput 17:2176–2214.

1047 Roelfsema PR, van Ooyen A, Watanabe T (2010) Perceptual learning rules based on reinforcers and attention.
1048 Trends Cogn Sci 14:64–71.

1049 Rutkowski RG, Weinberger NM (2005) Encoding of learned importance of sound by magnitude of
1050 representational area in primary auditory cortex. Proc Natl Acad Sci U S A 102:13664–13669.

1051 Saito DN, Yoshimura K, Kochiyama T, Okada T, Honda M, Sadato N (2005) Cross-modal Binding and
1052 Activated Attentional Networks during Audio-visual Speech Integration: a Functional MRI Study. Cereb
1053 Cortex 15:1750–1760.

1054 Schiffer AM, Muller T, Yeung N, Waszak F (2014) Reward activates stimulus-specific and task-dependent
1055 representations in visual association cortices. J Neurosci 34:15610–15620.

1056 Schultz W (2000) Multiple reward signals in the brain. Nat Rev 1:199–207.

1057 Seitz AR, Watanabe T (2009) The phenomenon of task-irrelevant perceptual learning. Vision Res 49:2604–
1058 2610.

1059 Serences JT (2008) Value-based modulations in human visual cortex. Neuron 60:1169–1181.

1060 Serences JT, Yantis S (2007) Spatially selective representations of voluntary and stimulus-driven attentional
1061 priority in human occipital, parietal, and frontal cortex. Cereb Cortex 17:284–293.

1062 Shapiro K, Hillstrom AP (2002) Control of visuotemporal attention by inferior parietal and superior temporal
1063 cortex. Curr Biol 12:1320–1325.

1064 Shuler MG, Bear MF (2006) Reward timing in the primary visual cortex. Science 311:1606–1609.

1065 Stanisor L, van der Togt C, Pennartz CMA, Roelfsema PR (2013) A unified selection signal for attention and
1066 reward in primary visual cortex. Proc Natl Acad Sci U S A 110:9136–9141.

1067 Stein BE, Stanford TR (2008) Multisensory integration: Current issues from the perspective of the single
1068 neuron. Nat Rev Neurosci 9:255–266.

1069 Stephan KE, Penny WD, Daunizeau J, Moran RJ, Friston KJ (2009) Bayesian model selection for group studies.
1070 Neuroimage 46:1004–1017.

1071 Stephan KE, Penny WD, Moran RJ, den Ouden HEM, Daunizeau J, Friston KJ (2010) Ten simple rules for
1072 dynamic causal modeling. Neuroimage 49:3099–3109.

1073 Tremblay L, Worbe Y, Hollerman JR (2009) The ventral striatum: A heterogeneous structure involved in reward
1074 processing, motivation, and decision-making. Handb Reward Decis Mak:51–77.

1075 Vakhrushev R, Cheng FP-H, Schacht A, Pooresmaeili A (2023) Differential effects of intra-modal and cross-
1076 modal reward value on perception: ERP evidence. PLoS One 18:e0287900.

1077 Watson AB, Pelli DG (1983) Quest: A Bayesian adaptive psychometric method. Percept Psychophys 33:113–

120.

Weil RS, Furl N, Ruff CC, Symmonds M, Flandin G, Dolan RJ, Driver J, Rees G (2010) Rewarding feedback after correct visual discriminations has both general and specific influences on visual cortex. J Neurophysiol 104:1746–1757.

Werner S, Noppeney U (2010) Distinct functional contributions of primary sensory and association areas to audiovisual integration in object categorization. J Neurosci 30:2662–2675.

Wilmes KA, Clopath C (2019) Inhibitory microcircuits for top-down plasticity of sensory representations. Nat Commun 10.

Zald DH, McHugo M, Ray KL, Glahn DC, Eickhoff SB, Laird AR (2014) Meta-Analytic Connectivity Modeling Reveals Differential Functional Connectivity of the Medial and Lateral Orbitofrontal Cortex. Cereb Cortex 24:232–248.

Zeidman P, Jafarian A, Seghier ML, Litvak V, Cagnan H, Price CJ, Friston KJ (2019) A guide to group effective connectivity analysis, part 2: Second level analysis with PEB. Neuroimage 200:12–25.

Zink CF, Pagnoni G, Chappelow J, Martin-Skurski M, Berns GS (2006) Human striatal activation reflects degree of stimulus saliency. Neuroimage 29:977–983.

Table Legends

Table 1. Behavioral results during the visual discrimination task performed in pre- and post-conditioning.

Table 2. Whole-brain activations of value decoders thresholded at uncorrected $p < .005$ and $k = 20$. Regions marked with bold font were selected as ROIs used for the effective connectivity analysis

Figure Legends

Figure 1. Behavioral paradigms. **A)** On the left side the visual discrimination task (VDT) used in the test phase (pre- and post-conditioing) is shown. Participants were instructed to discriminate the orientation of a Gabor patch (i.e. clockwise or counter-clockwise) by pressing upper or lower arrow keys on a response box, repectively. Simultaneously with the Gabor target, a task-irrelevant visual (intra-modal) or auditory (cross-modal) cue was also presented at the same location. The VDT task was employed both before and after a conditioing task (shown on the right side) where the reward associations of intra- and cross-modal cues were learned. During the conditioing, participants were asked to indicate whether the cues (auditory or visual) were presented to the left or right side (by pressing the left or right arrow keys on a response box, repectively). The properties of the cues (color for the visual and pitch for the auditory tone) predicted different magnitudes of reward that was shown on the display during a feedback phase. During VDT, intra- and cross-modal cues were never predictive of reward delivery and accordingly the feedback display only contained a fixation point. **B)** The sequence of tasks employed during the experiment for each participant: first the VDT was completed before the cues were associated with rewards

(referred to as the *pre*-conditioing phase recorded on day 1). Thereafter during the second session recorded on another day, participants first learned the reward associations of visual and auditory cues during the conditioing and then proceeded to the *post*-conditioning VDT with the cues that had been associated with rewards. To prevent the exinction of reward effects, the reward associations were reminded by interleaving the VDT with short conditioing blocks.

Figure 2. Behavioral and BOLD effects of reward on visual discrimination. A) Baseline corrected reaction times for all conditions. Horizontal lines in boxplots are the mean for each condition and each dot represents the data of one participant. **B)** Reward facilitation in early visual areas (masked with V1-V2 anatomical mask from Eickhoff and colleagues (2005)). The activations correspond to regions in area V1-V2 where the classification accuracy of the orientation decoder was higher for high compared to low reward condition during the post-conditioning after correcting for differences in pre-conditioning. Activations are shown at an uncorrected $p < .005$, $k = 10$, revealing a peak in the right hemisphere located at xyz = [9 -64 5] and in the left hemisphere at xyz = [-12 -67 2]. **C)** Reward facilitation shown in B occurred in V1-V2 regions that were responsible for the processing of the target. The cyan color illustrates the regions that were activated by the target (fMRI contrast: neutral stimulus versus baseline) thresholded at $p_{FWE} < .05$ and $k = 0$. The magenta color shows the reward-driven facilitation effect in visual areas thresholded at uncorrected $p < .005$, $k = 10$ (as in B). The cursor is at xyz = [9 -64 5]. See also the **Figure 2-1** and **Table 2-1** for the results of the univariate analysis of reward effects during the conditioning phase.

Figure 3. **Regions of interest identified by the value decoders and used for the effective connectivity analysis.** *Value decoder1* identified a cluster in the OFC xyz = [51 26 -7] shown in blue, which discriminated high and low value stimuli irrespective of their sensory properties (i.e., location and sensory modality). *Value decoder2,* classified high and low reward stimuli from each location and sensory modality separately and showed clusters in IPS xyz = [-33 -58 53] in green and STS xyz = [57 -28 8] in red, where reward value was reliably decoded across sensory modalities. The activations are shown at uncorrected $p < .005$ with $k = 20$, and the cursor is located at xyz = [48 -58 12] to illustrate all ROIs (see also **Figure 3-1**).

Figure 4. Effective connectivity results. A) Schematic of 11 models that were considered to probe the mode of the bidirectional communication between the reward-related areas and the early visual areas (EVA). **B)** The models were estimated for both pre- (in grey) and post-conditioning (in black) phases. The exceedance probabilities of random effects Bayesian model selection demonstrated that model 11 (null model) wins in pre- and model 10 wins in post-conditioning. **C)** Estimated parameters (in Hz) of the winning model in post-conditioning were used to characterize the reward modulation (i.e., changes in the strength of each connection when comparing high relative to low rewards) corrected for effects before reward associations were learned (i.e., post – pre-conditioning). Reward modulations are shown for each connection between two regions and separately for each direction (feedback

and feedforward, in teal and dark yellow, respectively). * corresponds to $p < 0.01$ (equivalent to posterior probabilities > 0.99) and corrected for multiple comparison using Bonferroni correction. Error bars depict the 99% confidence intervals of the subtracted distribution (high – low). The middle panel illustrates the schematic of the winning model and depicts the strength of the reward modulation for feedforward and feedback connections (teal and dark yellow arrows, respectively) and their respective posterior probability (in bracket) for the intra-modal (blue) and cross-modal (red) conditions.

Legends to Extended Data Figures

Figure 2-1. Main effect of reward (AH+VH>AL+VL, AH: Auditory High reward, VH: Visual High reward, AL: Auditory low reward and VL: Visual Low reward) during the conditioning phase. A) Contrast between high against low reward conditions, thresholded at $p < .001$ (uncorrected) with k = 10 and masked with an anatomical ROI encompassing the ventral striatum (i.e., Putamen, Caudate, and Globus Pallidus). Crosshair is at the peak activation xyz = [9 11 2]. B) Bar graphs depict the contrast estimates of high against low reward conditions. ** corresponds to $p < 0.01$ based on a paired sample *t*-test.

Figure 3-1. Whole-brain results of the value decoders depicting sagittal, coronal, and the axial view for: A) lateral orbitofrontal areas xyz = [51 26 -7] in the right hemisphere from *value decoder 1*. B) The left anterior intraparietal areas xyz = [-33 -58 53] and C) The right superior temporal areas xyz = [57 -28 8] detected by the *value decoder 2* across sensory modalities. These ROIs were taken further to the effective connectivity analysis. All images were thresholded at uncorrected $p < .005$, k = 20. The cursor is at the peak activities of each corresponding ROI coordinates written in brackets.

Legends to Extended Data Tables

Table 2-1. Whole-brain analysis result during conditioning phase with uncorrected threshold of $p < .001$ and extent threshold of k = 10.

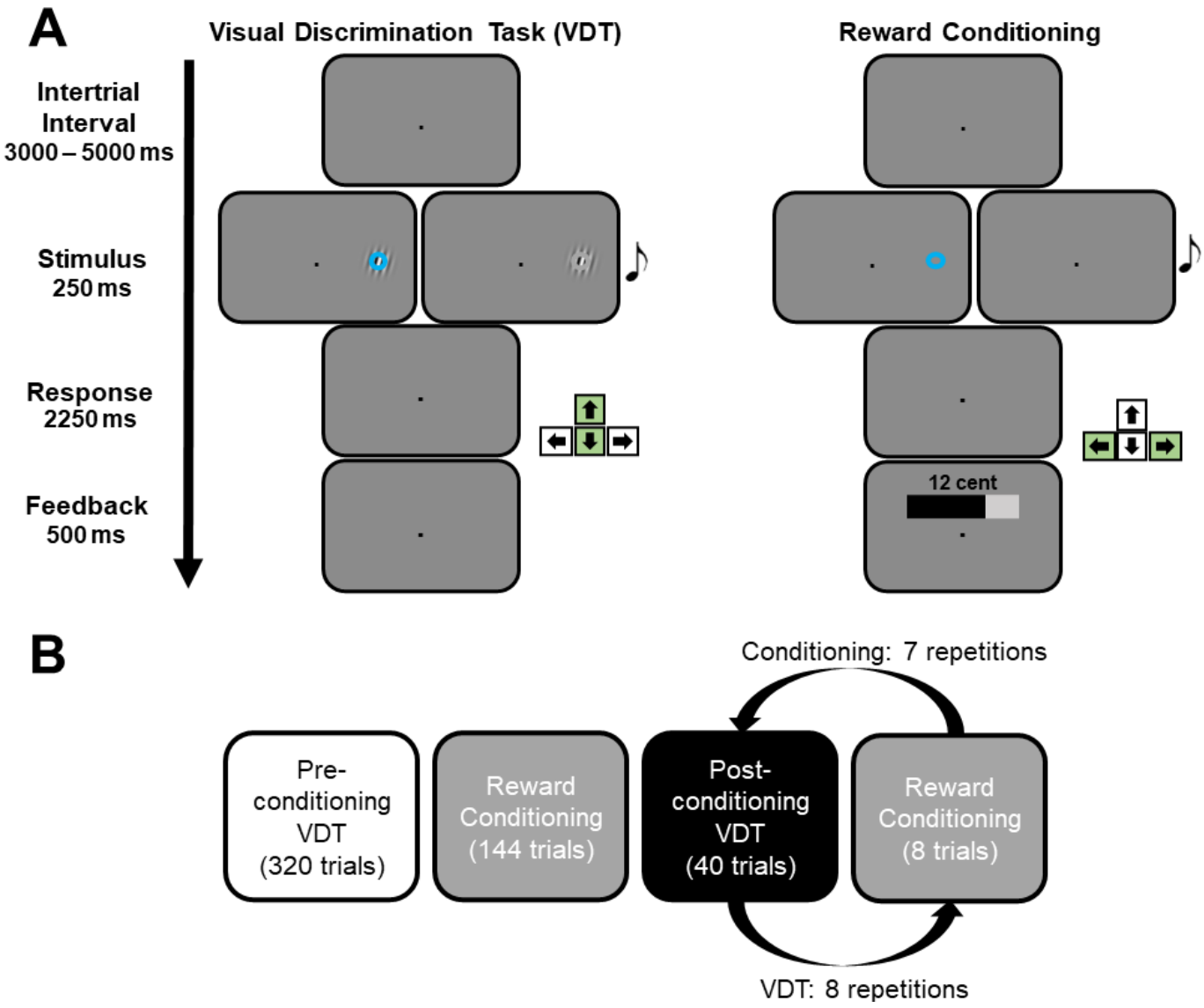

A

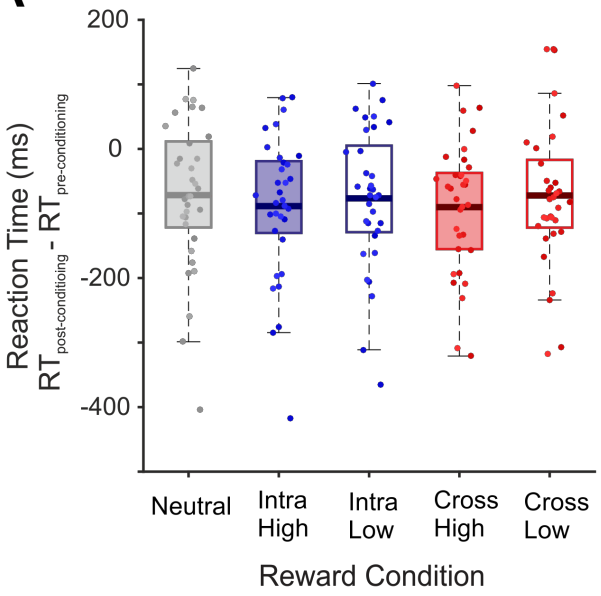

B

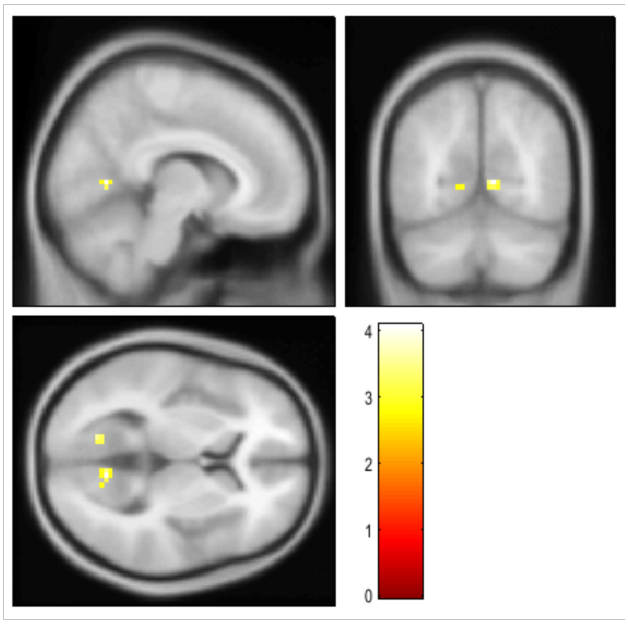

C

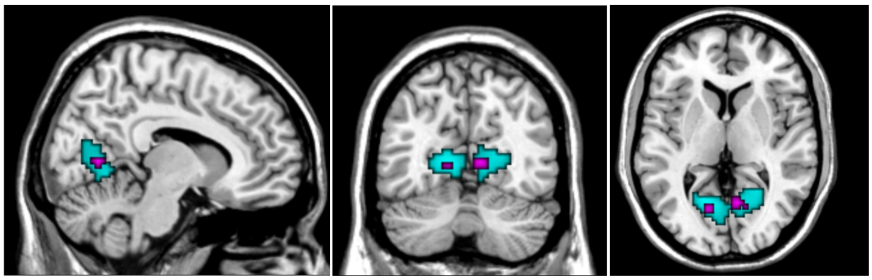

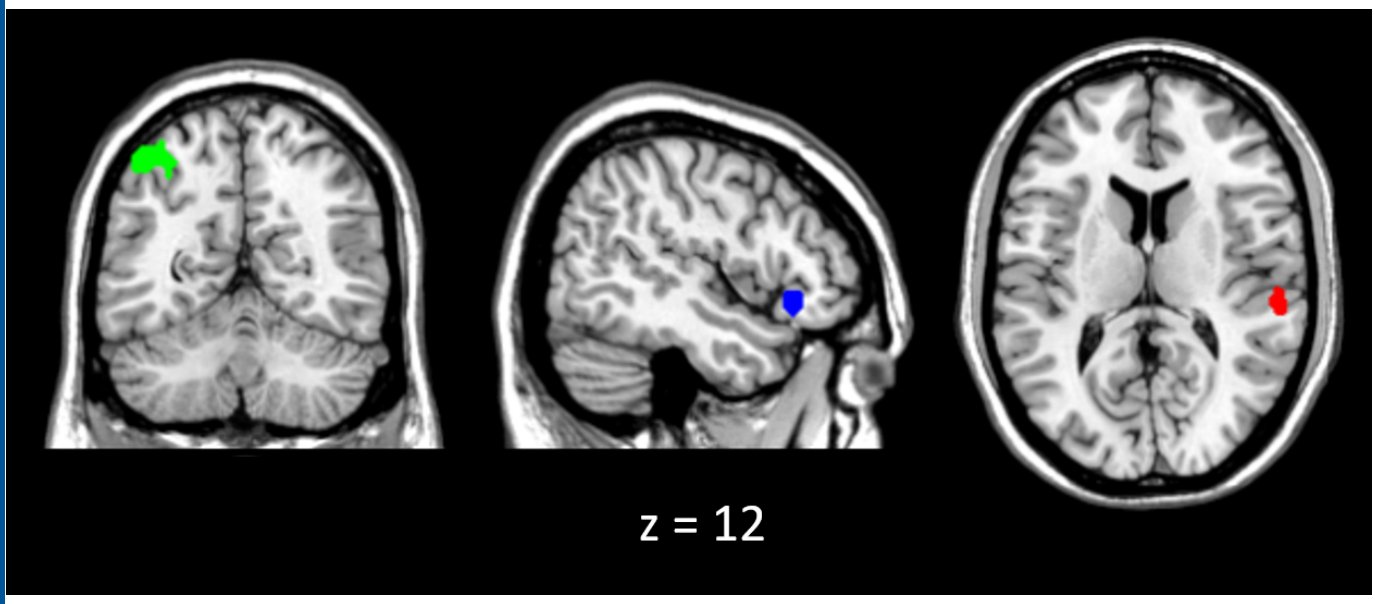

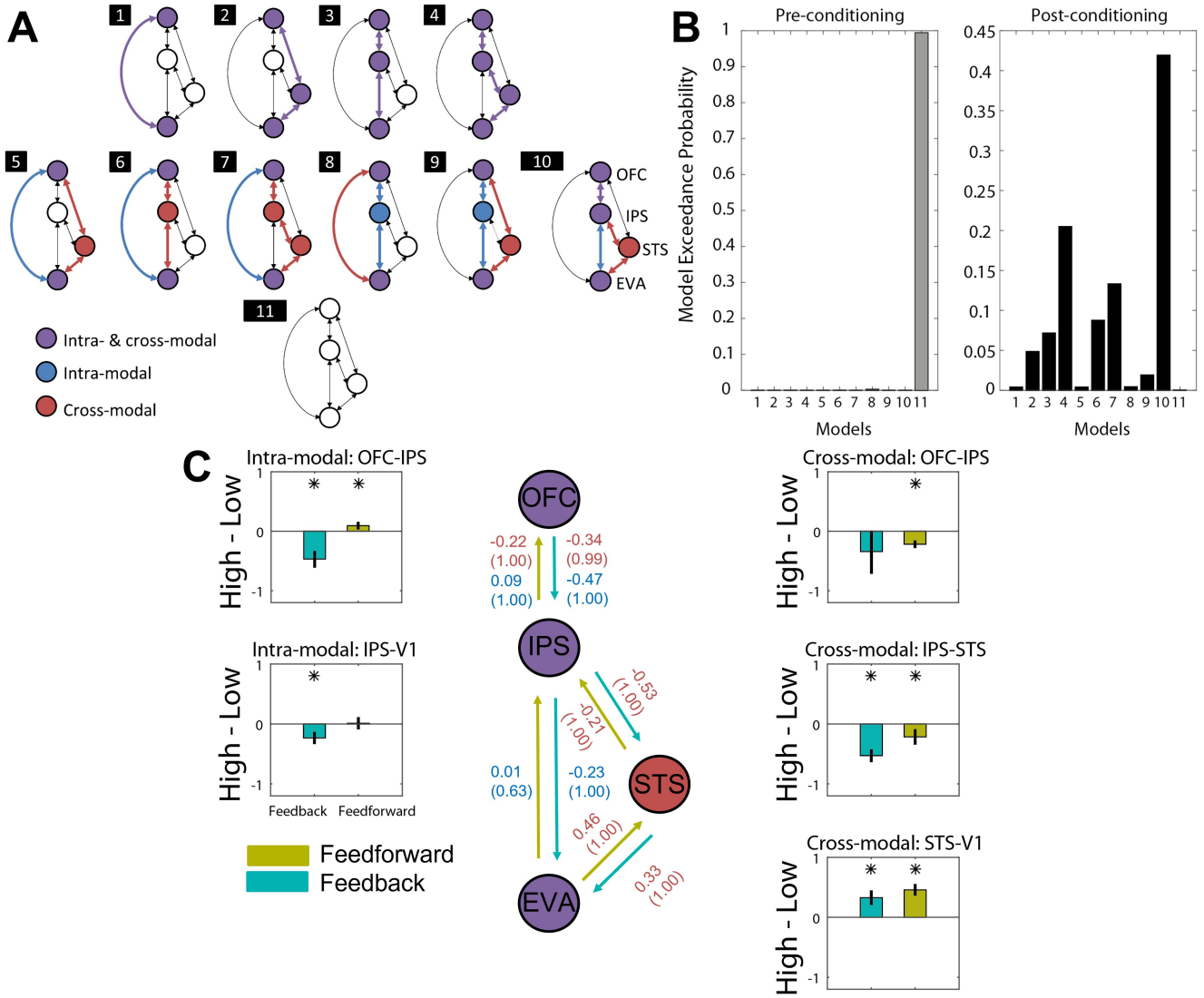

Table 1

Condition	**RT (pre-conditioning)**	**Accuracy (pre-conditioning)**	**RT (post-conditioning)**	**Accuracy (post-conditioning)**
High Reward Intra-modal (HV)	938.33±24.13 ms	81.08±1.09%	849.72±20.25 ms	80.53±1.33%
Low Reward Intra-modal (LV)	929.56±23.77 ms	80.80±1.29 %	852.98±19.71 ms	80.23±1.48%
High Reward Cross-modal (HA)	934.15±26.25 ms	82.25±1.07%	843.40±20.79 ms	82.25±1.38%
Low Reward Cross-modal (LA)	920.64±26.08 ms	84.48±1.71 %	848.50 ±21.59 ms	84.48±1.36%
Neutral	925.08±24.04 ms	80.68±1.40%	852.67±19.71 ms	80.66±1.60%

1 Table 2

Cluster size	**MNI coordinates (in mm)**			**T**	***p***	**Side**	**Region**
	x	y	z				
Results of *Value Decoder 1*: areas that distinguish between high and low value irrespective of sensory properties							
43	**51**	**26**	**-7**	**6.08**	**0.006**	**R**	**Inferior orbitofrontal**
44	-45	-46	-49	5.27	0.006	L	Cerebelum
80	36	-79	-52	4.69	0.000	R	Cerebelum
37	42	-61	-4	4.39	0.01	R	Inferior temporal
22	3	4	11	4.06	0.038	L	Caudate
23	12	8	41	3.64	0.034	R	Cingulate cortex
22	-42	23	-16	3.55	0.038	L	Inferior orbitofrontal
23	-3	65	-7	3.52	0.034	L	Medial orbitofrontal
Results of *Value Decoder 2*: areas that distinguish between high and low value for each location and sensory modality. After value classification was performed, results were inspected **across sensory modalities.**							
37	**57**	**-28**	**8**	**4.62**	**0.01**	**R**	**Superior temporal**
34	-6	-73	23	4.37	0.012	L	Cuneus
36	9	-37	44	4.35	0.01	R	Cingulate cortex
69	**-33**	**-58**	**53**	**4.03**	**0.001**	**L**	**Inferior parietal**
28	-18	-52	8	4.00	0.021	L	Precuneus
20	-51	44	-1	3.82	0.046	L	Inferior orbitofrontal
39	-12	-25	71	3.80	0.008	L	Motor cortex
24	21	-28	53	3.54	0.031	R	Somatosensory
22	-54	-55	26	3.40	0.037	L	Temporoparietal
23	-57	2	-1	3.28	0.034	L	Temporal pole
Results of *Value Decoder 2*: areas that distinguish between high and low value for each location and sensory modality. After value classification was performed, results were inspected for **intra-modal stimuli.**							
27	-12	-22	71	4.81	0.024	L	Paracentral lobule
20	57	-31	8	4.72	0.047	R	Superior temporal
23	45	-28	53	4.58	0.035	R	Postcentral
36	-36	-61	56	4.49	0.011	L	Superior parietal
32	-24	23	56	4.45	0.015	L	Frontal mid
28	3	50	32	4.12	0.022	R	Frontal sup medial
26	9	-55	-43	3.91	0.026	R	Cerebelum
20	-36	-76	-1	3.68	0.047	L	Occipital mid

21	-9	-82	-28	3.54	0.043	L	Cerebelum
22	-51	-64	-16	3.46	0.039	L	Inferior temporal
Results of *Value Decoder 2*: areas that distinguish between high and low value for each location and sensory modality. After value classification was performed, results were inspected for **cross-modal stimuli.**							
60	-39	-25	5	5.17	0.001	L	Heschl
37	54	-28	5	4.66	0.008	R	Superior temporal
20	48	-1	2	4.56	0.041	R	Insula
30	-6	-73	23	4.49	0.015	L	Cuneus
25	-66	-28	17	4.35	0.024	L	Superior temporal
41	-57	-55	29	4.24	0.006	L	Angular
66	12	-25	38	4.07	0.001	R	Cingulum mid
24	-42	5	-19	3.77	0.027	L	Temporal pole sup
27	-15	-46	-13	3.69	0.02	L	Fusiform
21	-18	-52	8	3.44	0.037	L	Calcarine
Results of *Value Decoder 2*: areas that distinguish between high and low value for each location and sensory modality. After value classification was performed, results were inspected for the interaction of **cross-modal>intra-modal.**							
36	-42	-19	5	3.78	0.009	L	Heschl gyrus
Results of *Value Decoder 2*: areas that distinguish between high and low value for each location and sensory modality. After value classification was performed, results were inspected for the interaction of **intra-modal>cross-modal.**							
No voxel survived							

2